Comparative study on quantitative carbon content mapping in archaeological ferrous metals with laserinduced plasma spectroscopy (LIBS) and nuclear reaction analysis (NRA) for 3D representation by LIBS

Xueshi Bai, Thomas Calligaro, Laurent Pichon, Brice Moignard, Quentin Lemasson, Manon Gosselin, Sarah Richiero, Philippe Dillmann, Florian Téreygeol, Jessica Auber–Le Saux, et al.

Comparative study on quantitative carbon content mapping in archaeological ferrous metals with laser-induced plasma spectroscopy (LIBS) and nuclear reaction analysis (NRA) for 3D representation by LIBS

Xueshi Bai[1,2], Thomas Calligaro[1,2,3], Laurent Pichon[1,2], Brice Moignard[1,2], Quentin Lemasson[1,2], Manon Gosselin[4,5], Sarah Richiero[1,6], Philippe Dillmann[5], Florian Téreygeol[5], Jessica Auber--Le Saux[1,6], Nicolas Wilkie-Chancellier[7], Vincent Detalle[1,2,3 *]

[1]Centre de Recherche et de Restauration des Musées de France (C2RMF), 14 quai François-Mitterrand, 75001 Paris, France.
[2]Centre National de la Recherche Scientifique (CNRS), Federation de recherche NewAGLAE FR3506, Paris,France.
[3]PSL Research University, Institut de Recherche Chimie Paris, Chimie ParisTech, CNRS UMR 8247, 75005 Paris, France
[4]CNRS, UMR7041, ArScAn, Equipe GAMA, MAE, Université de Nanterre, France
[5]LAPA-IRAMAT, NIMBE, CEA, CNRS, Université Paris-Saclay, CEA Saclay 91191 Gif-sur-Yvette, France
[6]Fondation des sciences du patrimoine/EUR-17-EURE-0021, Cergy-Pontoise cedex, France
[7]SATIE, Systèmes et Applications des Technologies de l'Information et de l'Energie, CY Cergy-Paris Université, ENS Paris-Saclay, CNRS UMR 8029, 5 mail Gay Lussac, 95031 Neuville sur Oise, France

[*] vincent.detalle@culture.gouv.fr

Abstract

The carbon content distribution of ferrous archaeological artefacts in a quantitative way allows us to understand the nature of the materials. Our previous works have ever proved that the use of laser-induced breakdown spectroscopy (LIBS) could be an efficient method to solve problems of in situ analysis and offer a high spatial resolution. To assess the ability of this quantification in an absolute way the carbon quantification by LIBS is compared in this paper with the nuclear reaction analysis (NRA), one of the ion beam analysis (IBA) techniques generated by a deuterium ion beam. The IBA analysis has specific advantages, especially in terms of precision and non-destructiveness. A validation study is also presented on quantitative carbon content mapping in archaeological ferrous metals with LIBS and deuterium ion beam analysis. The application of LIBS quantitative mapping on different structures of archaeological pieces shows that the carbon content distribution can be well determined, demonstrating the 2D mapping capabilities of the laser techniques. With the help of LIBS stratigraphic analysis, a 3D deeper insight on microscale features presents a heterogeneity, induced better understanding of material organization at the microscale.

Keywords: LIBS quantification of carbon concentration in steel, LIBS mapping and 3D tomography, archaeology, IBA

1. Introduction

Studying the metallurgies through archaeometallurgy, one of the major approaches to the history of techniques, allows us to understand from the nature of the production process to the commercial exchanges of the products of ancient societies in a holistic manner. For ferrous metals, carbon content is a decisive parameter to the mechanical behavior of the material [1]. This determination is particularly difficult for old ferrous alloys because of their heterogeneous distribution in the material. For example, different grain size, distribution, phase morphology, elemental segregation or local gradients in crystallographic orientation [2, 3] change the mechanical properties. Therefore, structural analytical methods, such as X-ray diffraction[4] and internal friction measurement [5], energy loss spectroscopy [6], electron backscatter diffraction [7], are needed to reveal the different phases of steel in order to deduce the carbon distribution. But the measurement is often carried out on a section surface after Nital etching where the latter appears as a discontinued structure made of raised retained austenite and eroded ferrite by different means with various spatial resolutions. Among them, the secondary electron microscopy or secondary ion mass spectroscopy (SIMS) can draw the carbon distribution with a micron resolution and the spatial resolution can reach sub-micron if a Nano-beam is used [8]. In addition, the wavelength dispersive electron probe microanalysis (EPMA) can measure carbon concentration in steel, which occupies an intermediate position where micrometer to nanometer structure can be characterized [9]. However, these techniques require heavy instruments, a vacuum environment, huge sample preparation and they cannot analyze a large area.

At present time, the most efficient method in terms of cost/sensitivity ratio is the metallographic analysis by optical microscopy after Nital etching [3, 10], by measuring the volume of the precipitated phases containing carbon and in particular cementite (Fe_3C). However, this classical quantitative metallographic analysis, after image processing, is based on thermodynamic considerations and only reliable at equilibrium state and suffers other important limitations. This method is relatively time-consuming as it requires observation and description by an experienced operator. It is difficult to implement for *in situ* observations and

it cannot be used directly on artwork or objects and lacks precision for some structures cooled down under the condition out of equilibrium (martensite, bainite, Widmanstätten).

Therefore, we have proposed in our previous work to use laser-induced breakdown spectroscopy (LIBS) as a new and efficient way to solve problems related to *in situ* analysis and to offer a high spatial and adaptive resolution. The use of LIBS allows the analysis of a large number of objects/samples, in the laboratory as well as on field, and to determine precisely and locally the carbon content and its variation in the object[11]. However, the LIBS quantitative analysis is a method needing a set of standard references for ensuring its implementation. Thus, an absolute quantitative analysis method is developed in this paper: ions beam analysis (IBA) - deuteron-induced γ-ray emission (DIGE) [12] as an intercalibration of LIBS method, aiming to assess the quality of our LIBS quantitative measurement. IBA method is an absolute quantitative analytical technique as the control of experimental conditions and the high quality of the data on nuclear reactions allow a sensitivity of a few ppm with an accuracy below the percent. The methods are evaluated for carbon content calibration by LIBS and IBA-DIGE technics and the carbon quantitative mapping by these two methods is presented. LIBS stratigraphical analysis ability shows more and more applications in 3D analysis[13, 14], but the results were usually presented in slice as a function of the depth, which makes it sometimes difficult to compare different compositions in the same place. So, a deeper insight in 3D on microscale features for the quantitative carbon content representation is proposed in order to better understand the internal element distribution in the material.

2. Samples and their properties

By the eutectoid transformation (solid-to-solid phase) during the steel fabrication in equilibrium state at constant temperature, , the austenite is transformed into cementite (Fe_3C) and ferrite (0.02% C) [15]. The obtained lamellar compound is called "pearlite", which contains 0.8% carbon. At the eutectoid temperature, several phases are formed, each with a different composition. The heterogeneity due to the high temperature heating would favor the oriented germination of the ferrite, then normal ferrite develops a needle-like crystallization called "acicular". These structures form regardless of the carbon content of the steel but are more difficult to obtain at low concentration [16].

Two different artefacts have been used in this work. The first one CL13286b is a cut in a wedge on the part of the left end of a semi-finished product. This semi-finished product is

closer to the finished object and dated from a period between the end of the 13th century and the beginning of the 14th century from the Castel-Minier site in Ariège, France. Its images after Nital etching of the cross-section shown in Fig. 1a, reveal that it has been made on an equilibrium state. The quantitative carbon mapping was performed on an archaeological artefact [17, 18] that proved a good performance of LIBS quantification to archaeological samples.

The second one CL12247-3 is a semi-product offcut (square bar), coming from the Castel-Minier site, in Ariège, French Pyrénées. It is dated from the XVth century and found around the castrum. The image after Nital etching of the cross-section of the sample CL12247-3 is shown in Fig. 1b. A Widmanstätten structure has been found with a typical acicular ferrite, which shows a fabrication on fast cooling state.

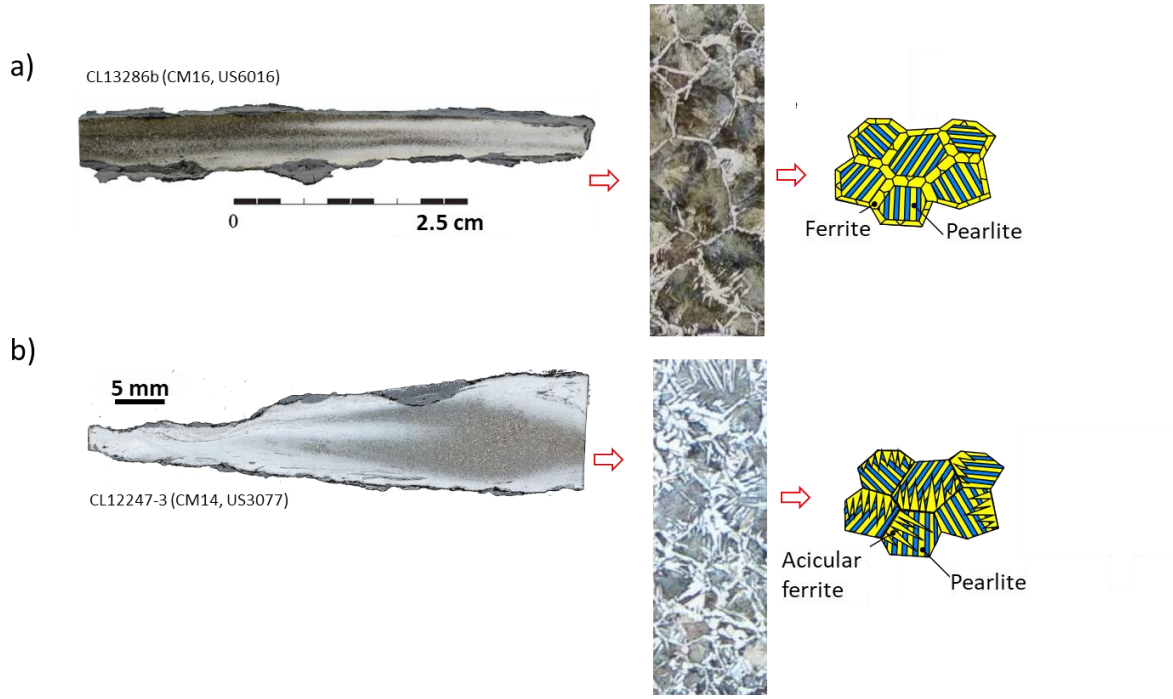

Fig. 1 The optical microscopic images after Nital etching of the cross section of archaeological samples. a) CL13286b (CM16, US6016) was on equilibrium state during the fabrication; b) CL12247-3 (CM14, US3077) has a Widmanstätten structure. Crystal structure of steels for slow cooling: distribution of ferrite (yellow) and cementite (blue) (https://fr.wikipedia.org/wiki/Acier, (2021)

In order to obtain the quantitative mapping, six reference steel samples were used to build a calibration curve for macro- and micro-analysis in previous works [19, 20]. They all have the equilibrium homogeneous phases with the carbon concentrations of 0.006%, 0.08%, 0.44%, 0.45%, 0.59% and 0.75%. The same series of these reference standard samples are used to carry out the IBA analysis to assess the LIBS quantification of carbon content in steel.

3. Experimental methods and measurements

3.1. IBA methods

IBA methods, compared to X-ray fluorescence, present several interesting aspects, in particular their capacity to measure light elements, including carbon, in a non-destructive manner. These characteristics have been used to analyze heritage materials [21]. Among the multiple IBA methods that allow the measurement of carbon, such as Elastic Recoil Detection Analysis (ERDA), non-Rutherford elastic backscattering (EBS) and NRA, the nuclear reaction between a deuterium ion (^{2}H or D) and a ^{12}C nucleus is the most often used. NRA has been carried out in the framework of an extensive work on the analysis of light elements [22] using deuteron beams and gamma detection with AGLAE accelerator[1]. This "stripping" nuclear reaction noted as ^{12}C(d,p gamma)^{13}C is very exo-energetic (Q-value = +2.72 MeV) and the high energy reaction products facilitate the detection at low background (protons at 2.7 MeV, gamma-ray of 3089 keV of the first excited level of the ^{13}C nucleus). The cross section of this reaction presents a maximum for incident deutons of 1.2 MeV. For thick targets, it is not interesting to use higher energy deutons, because this opens up reaction paths with other nuclei (traces of oxygen and nitrogen for example) whose reaction products can interfere with the measurement of ^{12}C and degrade the sensitivity of the method, and provoke radioprotection safety problems by neutron emission at the level of certain elements of the accelerator (slots and collimators in particular).

The carbon profile at depth is measured using the p0 proton group at 2.8 MeV and a surface barrier detector and this approach has already been applied for archaeological bronzes [23]. Previous works indicate a sensitivity for this DIGE analysis of the order of 0.1%[24], but one study indicates that it is possible to reach 100 ppm [25]. This detection limit depends on the composition of the matrix. In the case of an iron matrix, unlikely to induce reactions with deuterons, the required levels should be reached required for the analysis of carbon in ferrous alloys (concentration lower than 1%).

[1] Accélérateur Grand Louvre d'analyse élémentaire (AGLAE) is a particle accelerator housed by the Center for Research and Restoration of Museums of France in the Louvre museum in Paris, France.

3.2.LIBS and DIGE experimental setups

LIBS experiments are carried with macro and micro-analysis laser beams as described in our previous work[20]. The LIBS setup is shown in Fig. 2a. The ns laser beam of Nd:YAG at 1064 nm was focused on the sample surface with a diameter of about 50 µm for the micro-mapping and 220 µm for macro-analysis. The laser pulse energy was adjusted to keep the same laser fluence at 33.2 J/cm^2 for these two analysis configurations. In order to avoid interference with iron [26], the carbon peak at 193 nm was selected to extract the intensity of carbon emission. A mixture of argon and helium gas was guided to the sample surface in order to remove the impact of carbon present in the air and to less energy lost by its absorption, and also to optimize the signal-to-noise ratio [26, 27].

The calibration curve was built with averaged spectra of 230 laser shots of macro-analysis with 220 µm, the first 20 laser shots were used to remove the polluted surface. The calibration curve for micro-analysis with a 50 µm laser beam, was built with averaged spectra of 230 laser shots from a total of nine analyzed points in order to take account of the heterogeneity in this microscale, the first 20 laser shots for each point were used to remove the polluted surface.

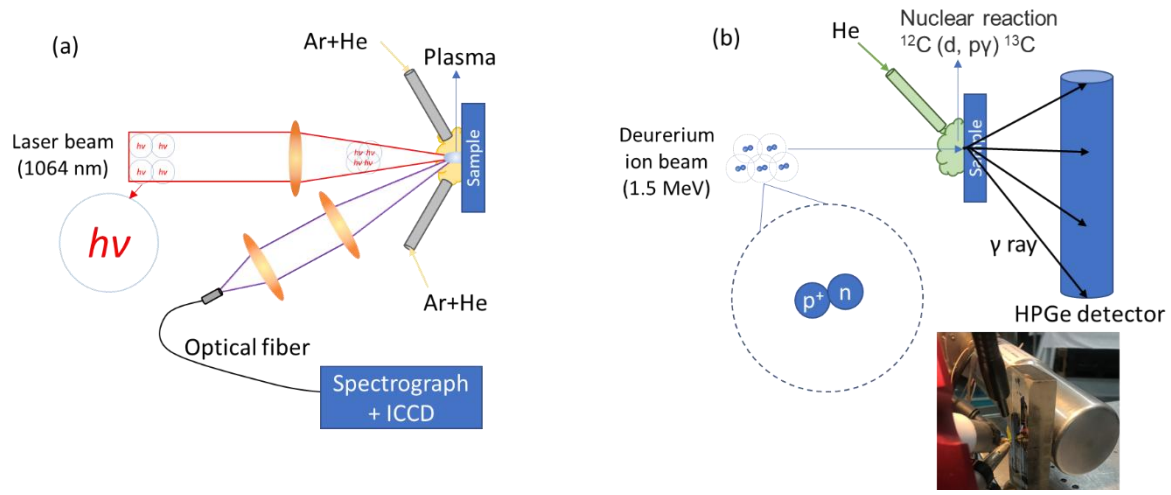

Fig. 2 Experimental setup: (a) LIBS setup; (b) IBA of deuterium setup with the insert photography of the setup in the laboratory.

Fig. 2b shows the IBA-DIGE experimental setup with the insert photography of the setup in the laboratory under AGLAE accelerator. The deuterium ion beam with a 1.5 MeV energy has an interaction zone of 50 µm diameter on the sample surface. This energy of deuterium ion was optimized for the nuclear reaction ^{12}C (d, pγ)^{13}C. The gamma ray emissions are collected

from the nuclear reaction by a HPGe detector. The position of the gamma-ray detector is several millimeters behind the samples and the gamma line is exploited at 3089 KeV [21]. A 5 L/min He flux is used to provide an environment in order to less energy lost by absorption in air.

Typical gamma spectra from pure carbon sample and two reference samples excited by deuterium ion beam are shown in Fig. 3. With the deuterium ions energy used, the detection shows the ability of a quantification measurement of carbon content in the range of 0.02% - 0.8%.

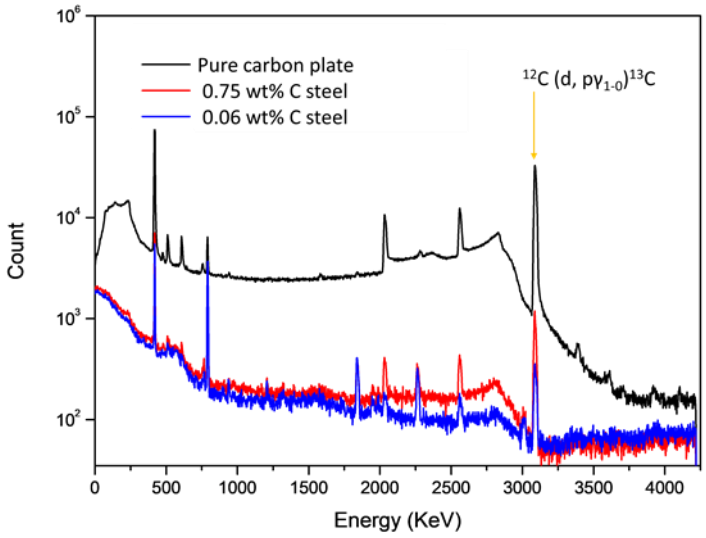

Fig. 3 Gamma spectra form pure carbon sample and two of reference sample excited by deuterium ion beam in He. The yellow arrow shows the gamma peak from carbon in reaction ^{2}C (d, pγ_{1-0})^{13}C

4. Results and discussion

4.1. Calibration curves and quantitative analysis abilities

Several measurements are performed on the same standard reference samples used in LIBS calibration measurement with deuterium ions scanning over a surface of 0.5 mm×0.5 mm with a total number of ions with a charge of 7.6 C for a duration of 5 mins for each sample. Then the counts read by HPGe detector are normalized in order to put in the same figure with the calibration curves by LIBS shown in Fig. 4.

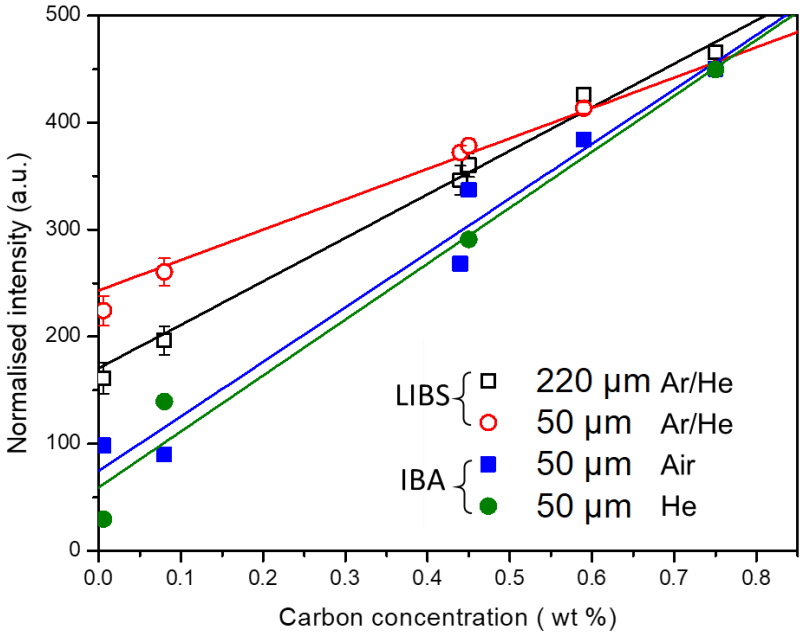

Fig. 4 Calibration curves of macro-LIBS under He/Ar atmosphere with 220 µm of averaged 230 laser shots at one spot, micro-LIBS with 50 µm of averaged 230 laser shots at one spot over nine spots, and deutons ions beams in different gas environment.

The linear regression and the coefficient of determination (R^2) are listed as follows:

$$I_{220\ \mu m\ laser} = 427.33(\pm 12.67)c\% + 160.42(\pm 4.36)\ ;\ R^2_{220\ \mu m\ laser} = 0.996$$

$$I_{50\ \mu m\ laser} = 284.06(\pm 17.07)c\% + 243.18(\pm 9.70)\ ;\ R^2_{50\ \mu m\ laser} = 0.991$$

$$I_{Air\ Deutons} = 509.14(\pm 43.97)c\% + 74.61(\pm 20.57)\ ;\ R^2_{Air\ Deutons} = 0.964$$

$$I_{He\ Deutons} = 522.59(\pm 59.76)c\% + 59.19(\pm 26.24)\ ;\ R^2_{He\ Deutons} = 0.961$$

As confirmed by statistics, the more analyzed points used to build the calibration curve, the more accurate the result will be [28]. So, the coefficients of determination of LIBS quantification are greater than that from IBA- DIGE, by the reason that we averaged 230 laser shot measurement for the macro-analysis and more than 2000 laser shots (230 × 9 points) for the micro-analysis, on the contrary, IBA-DIGE method is performed by scanning one big area for each sample. But the slope of the linear regression equation reflects the dynamic of carbon line directly link to the volume that has been analyzed. This analyzed volume is induced by total energy deposited on the surface (0.65 mJ for micro-LIBS and 12 mJ for macro-LIBS in our experiments for each laser pulse), in the case of laser sources. Although we kept the same

laser fluence, the spatial Gaussian profile of laser beam gave more intensity in the center of the 50 µm laser beam, which makes the micro-LIBS penetrated deeper in the steel than macro-LIBS. The IBA-DIGE measurements under air and He have the same slope, the same sensitivity of quantification, which shows the advantages of this method by nuclear actions.

The crater depth is estimated at about 17 µm for macro-analysis and 37 µm for micro-analysis [20]. As a result, the penetration depth for one shot is about 68 nm for macro-LIBS and 0.15 µm for micro-LIBS, which means the depth resolutions, respectively. Considering the conic form of the crater, the volume for macro-LIBS is estimated to be about 2.154×10^{-7} cm^3 for 250 laser shot measurements, 8.62×10^{-10} cm^3 for one shot ablation.

The 1.5 MeV deuterium ion beam can penetrate the sample about 6 µm [22], so the volume of analyzed material for building calibration curves is estimated at about 1.5×10^{-6} cm^3.

So, the total analyzed volume for LIBS is still about seven times fewer than that of DIGE, the quantification performs better with more quantity matter analyzed.

4.2. Mapping for archaeological samples

The mapping study is carried out with the same experimental setups and conditions used for the calibration curve on archaeological samples by LIBS and IBA-DIGE. The carbon quantitative mapping by IBA-DIGE was carried out with a resolution of 50 µm.

The micro-LIBS and IBA-DIGE mappings on the archaeological piece (CL13286b) with the equilibrium states reveal the carbon content distribution in Fig. 5, with the corresponding optical image of the section after Nital etching. It must be reminded here that the laser beam analyzed the area with a diameter of 50 µm, same as the deuterium beam. The step between two examined points gave a 100 µm spatial resolution of this mapping but it can help to avoid the possible pollution from the deposits of material of the plasma. The implementation of the DIGE induced the complete recovering of the surface with a step to step dimension equal to the spot dimension contrary to the libs that has a step of 100 micron that can induced a lost part of the grain borders, in some cases.

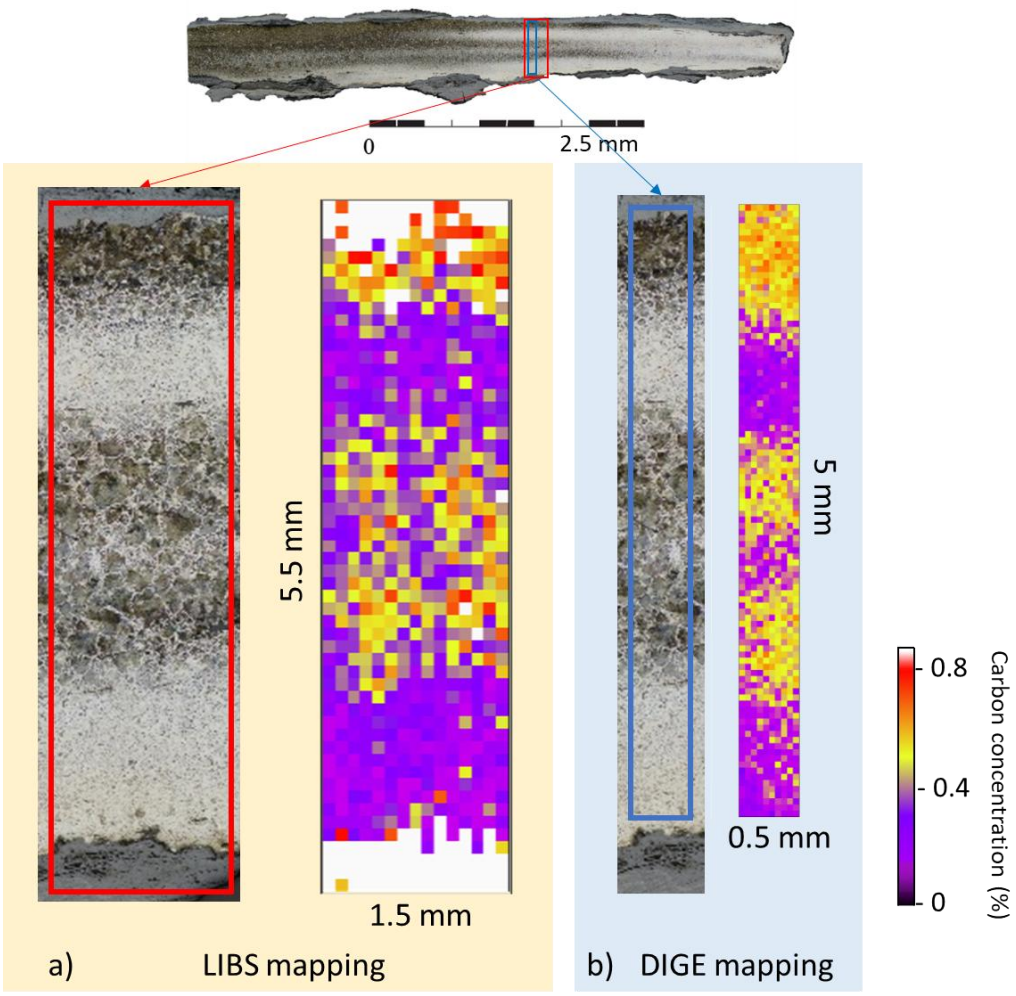

Fig. 5 Micro-LIBS and IBA-DIGE mapping on the archaeological piece CL13286b (CM16, US6016) with the equilibrium states

Table 1 resumes the mapping area, spatial resolution and time-consuming by macro and micro-LIBS [19] and IBA-DIGE methods . If the measuring area is extended for IBA-DIGE to the same as micro-analysis, the time consuming will reach the same duration for these two methods. The advantage of LIBS is that a mapping can be quickly performed with a low spatial resolution in order to look for the most concentrated carbon area.

Table 1 Mapping parameters on the archaeological piece with the equilibrium states

	Macro-LIBS	**Micro-LIBS**	**IBA ($^{2}H^{+}$)**
Mapping area (mm)	3× 6	1.5× 5.5	0.5× 5.5
Resolution (µm)	300	100	50
Time consuming	3 hours (120 shots/point)	4 hours (250 shots/point)	1 hours 30 mins

Two micro-LIBS mapping are carried out on the archaeological piece with Widmanstätten structure over an area of 1.8 mm×10 mm. It has been proved that if the steel material equivalent to the 50 single-shot volumes is analyzed, in this case, the results are efficient to get a quantitative mapping describing the distribution of carbon. Then 120 shots are used for each point analysis in order to keep the time consuming within 6 hours for each mapping measurement and 100 µm between two analyzed points. Fig. 6 shows the carbon distribution on these two areas based on 100 laser shots for each point by removing the first 20 shots in case of surface pollution (20 shots in our experimental condition remove about 3 µm of the material surface [20]). The carbon content distributions are different, although the optical images for these two areas are similar. It confirms in this case, LIBS enable us to get carbon concentration with a sufficient accuracy allowing a direct comparison to the metallographic analysis by observing optical microscopic images after Nital etching for Widmanstätten structure steel.

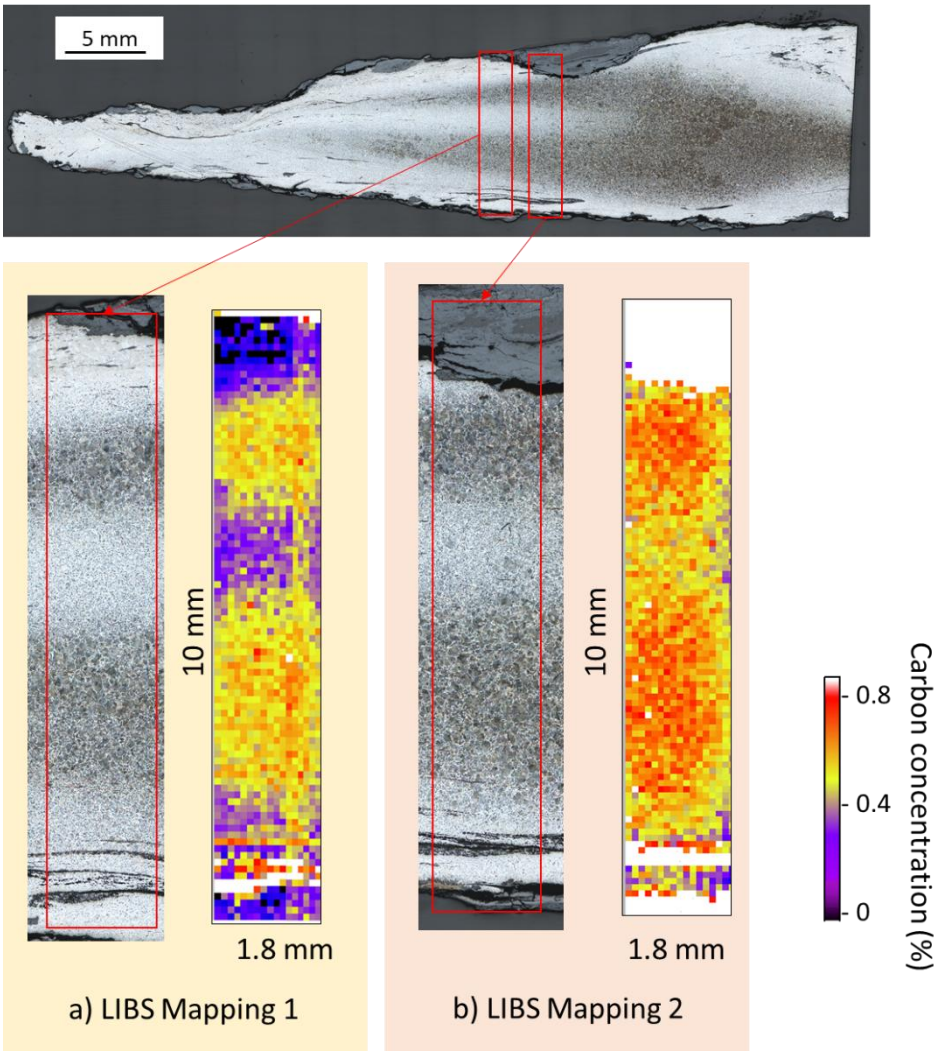

Fig. 6 Two micro-LIBS mapping images on the archaeological piece CL12247-3 (CM14, US3077) with Widmanstätten structure

4.3. 3D microscale insights by LIBS

One of the major advantage of LIBS is presented by its ability to ensure a concentration stratigraphic profile of each element without moving the sample. This capacity, could give to the analyst or the specialist of material a new point of view of its studied material. In our case, several laser shots at the same location allow us to access information on the distribution of carbon at depth, i.e. within the sample. [29]. Therefore, we separated the laser shots in-depth into different layers, and each laser contains 10 laser shots, so the thickness of each one is about 1.5 µm. The carbon concentration is calculated by a mean of these ten spectra, then we can get a carbon concentration distribution cube. Taking the piece CL13286b as an example, this carbon distribution cube is shown in Fig.7a as a top view and Fig. 7b as a 3D view with the proportional dimension of the real size. The depth of about 37 µm is not observable by comparing the surface size, but if we zoom into each point, the variation of carbon concentration as a function of the depth is revealed. In this dimension close to the micron, we may examine the variation inside of grains.

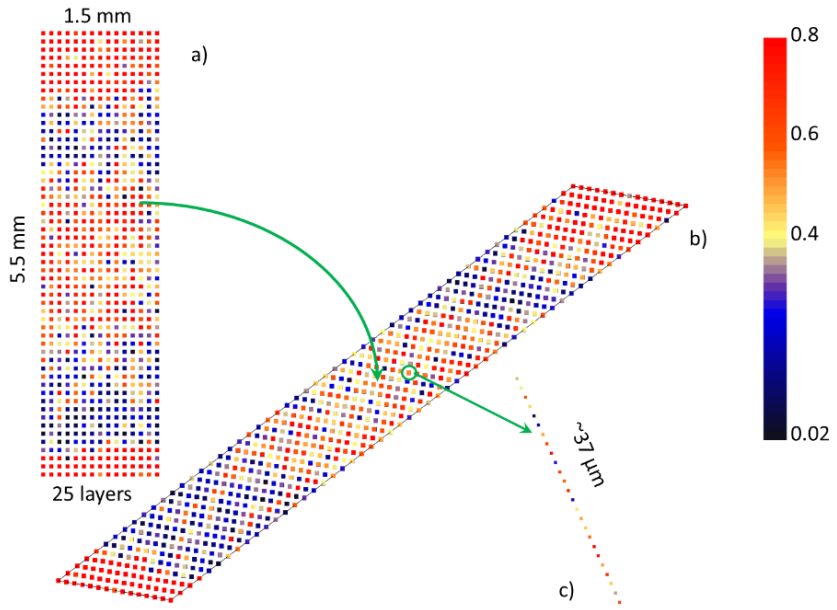

Fig. 7 Micro-LIBS on the archaeological piece CL13286b (CM16, US6016) in-depth into different layers, for each layer, the carbon concentration is calculated by the averaged of ten laser shots. The top view (a) and 3D view (b) of carbon concentration distribution cube with the proportional dimension of the real size; c) stratigraphy of one point in the carbon concentration distribution cube.

In order to have a better observation, the dimension of the depth is stretched as presented in Fig. 8a, the surface is marked with a green dot-line, and the arrow indicated the depth direction. Then the different carbon concentrations can be yielded by its distribution: the pearlite or close to pearlite (>0.75% C) in Fig. 7b, the normal steel content (0.45%C) in Fig. 7c and ferrite (0.02% C) or close to ferrite (0.02% - 0.1%C) in Fig. 7d. The corroded parts on the two sides contain more carbon with more than 0.8%, which dissolve the steel phases, on the contrary, inside the body, the different carbon distribution in a scale of a micron can be identified.

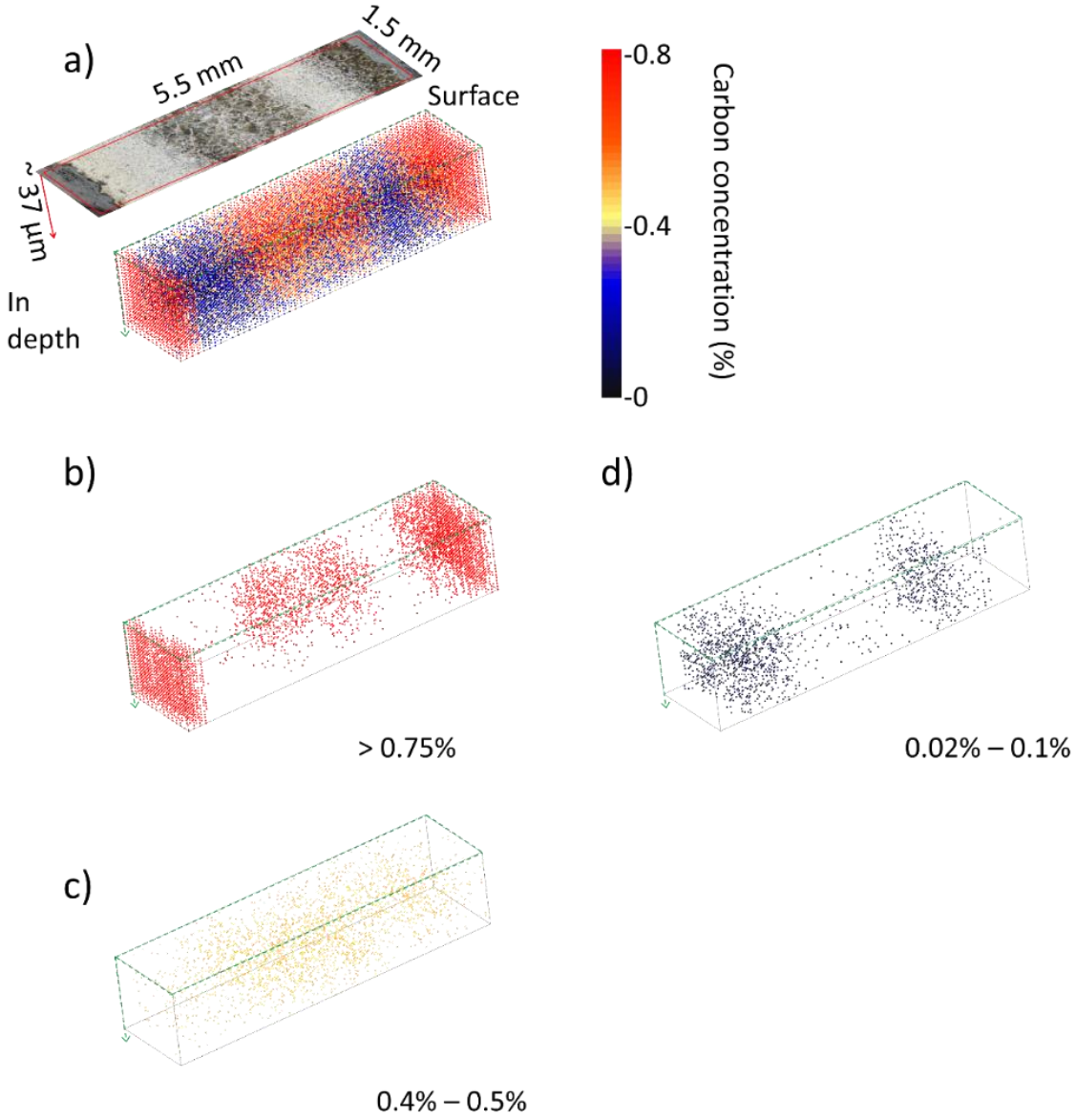

Fig. 8 Micro-LIBS volume analyses on the archaeological piece CL13286b with equilibrium state with 3D representation in different carbon concentration range: a) >0.02%; b) >0.75%; c) 0.4% - 0.5%; d) 0.02-0.1%. The surface is marked with green dot-line, and the arrow indicated the depth direction.

The carbon concentration distribution cubes of the archaeological piece of Widmanstätten structure for two analyzed zones are shown in Fig. 8. For each layer, the carbon concentration is calculated by the averaged of ten laser shots. The different carbon distribution for these two parts reveals that in the same piece and the same steel structure, the various orientation or size of grains give different carbon concentrations in depth. The 3D insight for these two parts present the distributions of pearlite as the main carbon composition corresponds to the optical image. In addition, the 3D insight brings to light other composition distribution: more ferrite in the part of Mapping 2 and more "normal steel" phase is presented in the part of Mapping 1.

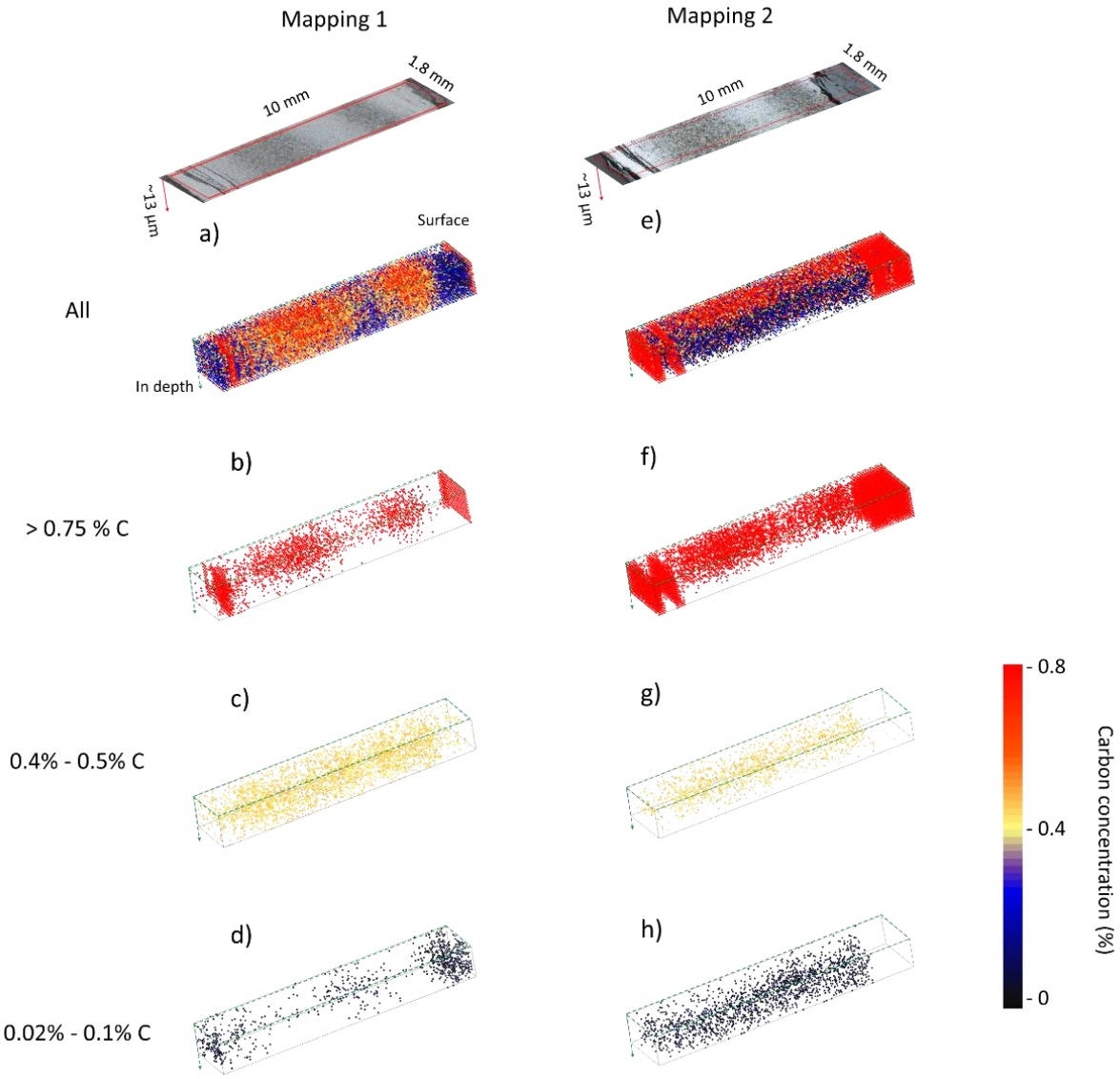

Fig. 8 3D view different carbon concentration of micro-LIBS volume analyses on the archaeological piece CL12247-3 with Widmanstätten structure for two mapping areas (a)-d) for Mapping 1 and e)-f) for Mapping 2) with different concentration range: a) >0.02%; b) >0.75%; c) 0.4% - 0.5%; d) 0.02-0.1%. The surface is marked with a green dot-line, and the arrow indicated the depth direction.

The capability of LIBS to perform tomographic quantitative elemental analysis is demonstrated. This aspect opens for general analytical science new possibilities to access information about material in term of 3D spatial element distribution at the level of micro or sub-microscale depending on the material physical/mechanical properties. This perspective is an open domain that could be directly implementable on site, close to the archeological site for example with often high polluted materials but as well corroded. In addition, this could be optimized in laboratories to be include in a 3D model of a sample or of an object.

5. Conclusions

Heritage sciences deal with questions of conservation or restoration for artworks or archaeological objects about their provenance, history, etc., which requires archaeometric analyses for the first representation of data and of mediation.

Among the various fields of heritage sciences, the archaeology occupies an important place, of which the metals and particularly the history of iron/steel, are widely studied because they compose the armors of soldiers, the clips of historical monuments, etc...

The analysis of the steel and especially its carbon content allows us to access the manufacturing technique and to determine the production periods. For this reason, a quantitative analysis is necessary to describe the concentration of carbon and its distribution within an object.

In this paper, we have demonstrated that carbon quantitative mapping and 3D microscales features described by LIBS is sensitive enough for detecting low carbon concentration in archaeological steel samples with phases in equilibrium state and even Widmanstätten structure as well.

We compared the calibration curves obtained by LIBS and a reference IBA-DIGE method that can give an absolute quantitative measurement of carbon concentration. IBA- DIGE provides direct quantitative mapping with a higher statistic ability and sensitivity with a shorter acquisition time but requires a large and not easy to access facility as AGLAE. This comparative study enables us to better understand the capability of LIBS quantification that has a direct relation with the laser energy of each single pulse deposited on the sample surface, which determines the analyzed material mass. LIBS quantification mapping gives several advantages in terms of mobility and the large area mapping analysis.

In addition, we proved the ability of LIBS to identify, in terms of real implementation of tomography representation, the repartition of different carbon concentration, allowing us to get the possibility to access to material organization in 3D dimensions. This representation in 3 dimensions of the internal structures of metals gives us access to a new way of apprehending and knowing better the materials, including dimension of aggregates and 3D diffusion of specific elements then deducing in better way the history of the objects and also their fabrications.

Acknowledgements

This work has been supported by the French Ministry Research Programs: EquipEx PATRIMEX (ANR-11-EQPX-0034) and ESR ESPADON-PATRIMEX (ANR-21-ESRE-00050). This work has also been supported the DIM MAP of the Ile de France Region. The research work was carried out with the support of a grant under the Decree of the Government of the Russian Federation No. 220 of 09 April 2010 (Agreement No. 075-15-2021-593 of 01 June 2021).

CRediT author statement

Xueshi Bai: Methodology, Software, Validation, Formal analysis, Investigation, Resources, Data Curation, Writing - Original Draft, Visualization. **Thomas Calligaro**: Conceptualization, Methodology, Validation, Formal analysis, Investigation, Resources, Writing - Review & Editing, Supervision. **Laurent Pichon**: Software, Formal analysis, Investigation, Resources, Data Curation. **Brice Moignard**: Resources. **Quentin Lemasson**: Investigation, Resources. **Manon Gosselin**: Resources. **Sarah Richiero**: Investigation. **Philippe Dillmann**: Conceptualization, Methodology, Resources. **Florian Téreygeol**: Resources. **Jessica Auber--Le Saux**: Investigation. **Nicolas Wilkie-Chancellier**: Resources. **Vincent Detalle**: Conceptualization, Methodology, Validation, Formal analysis, Resources, Writing - Original Draft, Visualization, Supervision, Project administration, Funding acquisition.

All authors have participated in Writing - Review & Editing.

Reference

[1] M.F. Ashby, D.R.H. Jones, Engineering materials: An introduction to their properties and applications, in, Pergamon press, Oxford, 1996.

[2] R. Pleiner, Iron in archaeology: the European bloomery smelters, Archeologický ústav AVČR, 2000.

[3] G. Pagès, P. Dillmann, P. Fluzin, L. Long, A study of the Roman iron bars of Saintes-Maries-de-la-Mer (Bouches-du-Rhône, France). A proposal for a comprehensive metallographic approach, J Archaeol Sci, 38 (2011) 1234-1252.

[4] L. Cheng, A. Böttger, T.H. De Keijser, E. Mittemeijer, Lattice parameters of iron-carbon and iron-nitrogen martensites and austenites, Scr Metall Mater, 24 (1990) 509-514.

[5] F. Pickering, The structure and properties of bainite in steels, (1967).

[6] C. Scott, J. Drillet, A study of the carbon distribution in retained austenite, Scripta Materialia, 56 (2007) 489-492.

[7] R. Petrov, L. Kestens, A. Wasilkowska, Y. Houbaert, Microstructure and texture of a lightly deformed TRIP-assisted steel characterized by means of the EBSD technique, Materials Science and Engineering: A, 447 (2007) 285-297.

[8] J.-B. Seol, B.-H. Lee, P. Choi, S.-G. Lee, C.-G. Park, Combined nano-SIMS/AFM/EBSD analysis and atom probe tomography, of carbon distribution in austenite/ε-martensite high-Mn steels, Ultramicroscopy, 132 (2013) 248-257.

[9] P.T. Pinard, A. Schwedt, A. Ramazani, U. Prahl, S. Richter, Characterization of dual-phase steel microstructure by combined submicrometer EBSD and EPMA carbon measurements, Microsc Microanal, 19 (2013) 996-1006.

[10] G.F. Vander Voort, S.R. Lampman, B.R. Sanders, G.J. Anton, C. Polakowski, J. Kinson, K. Muldoon, S.D. Henry, W.W. Scott Jr, ASM handbook, Metallography and microstructures, 9 (2004) 44073-40002.

[11] V. Detalle, X. Bai, The assets of laser-induced breakdown spectroscopy (LIBS) for the future of heritage science, Spectrochim Acta Part B, (2022) 106407.

[12] G.Á. Szíki, I. Uzonyi, E. Dobos, I. Rajta, K.T. Biró, S. Nagy, Á. Kiss, A new micro-DIGE set-up for the analysis of light elements, Nucl Instrum Methods Phys Res B, 219 (2004) 508-513.

[13] G.S. Senesi, B. Campanella, E. Grifoni, S. Legnaioli, G. Lorenzetti, S. Pagnotta, F. Poggialini, V. Palleschi, O. De Pascale, Elemental and mineralogical imaging of a weathered limestone rock by double-pulse micro-Laser-Induced Breakdown Spectroscopy, Spectrochim Acta Part B, 143 (2018) 91-97.

[14] R. Grassi, E. Grifoni, S. Gufoni, S. Legnaioli, G. Lorenzetti, N. Macro, L. Menichetti, S. Pagnotta, F. Poggialini, C. Schiavo, Three-dimensional compositional mapping using double-pulse micro-laser-induced breakdown spectroscopy technique, Spectrochim Acta Part B, 127 (2017) 1-6.

[15] ASM Handbook: Mechanical testing and evaluation, in, ASM International, 2000.

[16] Fe-C phase diagram for carbon steels, https://enwikipediaorg/wiki/Steel, (2021).

[17] P. Dillmann, F. Téreygeol, C. Verna, Premières analyses métallographiques des produits sidérurgiques trouvés sur le site médiéval de Castel-Minier (Aulus-les-Bains, 09), ArcheoSciences Revue d'archéométrie, (2006) 7-14.

[18] F. Téreygeol, Le Castel-Minier (Aulus-les-Bains), rapport intermédiaire, in, DRAC Midi-Pyrénées, 2016.

[19] X. Bai, M. Gosselin, P. Dillmann, F. Téreygeol, H. Allégre, J. Auber--Le Saux, V. Detalle, Quantitative mapping of carbon content in archaeological ferrous metals with laser-induced breakdown spectroscopy, SPIE, 2021.

[20] X. Bai, H. Allègre, M. Gosselin, P. Dillmann, M. Lopez, F. Téreygeol, V. Detalle, Impact of laser-induced breakdown spectroscopy implementation for the quantification of carbon content distribution in archaeological ferrous metals, Spectrochim Acta Part B, 172 (2020) 105964.

[21] T. Calligaro, J.-C. Dran, Art and Archaeology Application, in: M. Nastasi, J.W. Mayer, Y. Wang (Eds.) Ion beam analysis: fundamentals and applications, Taylor&Francis, 2014, pp. 267-307.

[22] Z. Elekes, A. Kiss, I. Biron, T. Calligaro, J. Salomon, Thick target γ-ray yields for light elements measured in the deuteron energy interval of 0.7–3.4 MeV, Nucl Instrum Methods Phys Res B, 168 (2000) 305-320.

[23] E. Ioannidou, D. Bourgarit, T. Calligaro, J.-C. Dran, M. Dubus, J. Salomon, P. Walter, RBS and NRA with external beams for archaeometric applications, Nucl Instrum Methods Phys Res B, 161 (2000) 730-736.

[24] G. Martin, G. Raveu, P. Garcia, G. Carlot, H. Khodja, I. Vickridge, M. Barthe, T. Sauvage, Quantitative ion beam analysis of M–C–O systems: application to an oxidized uranium carbide sample, Philos Mag, 94 (2014) 1177-1191.

[25] A. Ene, I. Popescu, T. Badica, Determination of carbon in steels using particle-induced gamma ray spectrometry, Journal of optoelectronics and advanced materials, 8 (2006) 222-224.

[26] J. Aguilera, C. Aragon, J. Campos, Determination of carbon content in steel using laser-induced breakdown spectroscopy, Appl Spectrosc, 46 (1992) 1382-1387.

[27] J. Aguilera, C. Aragon, A comparison of the temperatures and electron densities of laser-produced plasmas obtained in air, argon, and helium at atmospheric pressure, Appl Phys A, 69 (1999) S475-S478.

[28] J.-M. Mermet, Limit of quantitation in atomic spectrometry: An unambiguous concept?, Spectrochim Acta Part B, 63 (2008) 166-182.

[29] V. Detalle, Analyse de l'homogénéité du combustible nucléaire MOX par Spectrométrie d'Emission optique sur Plasma Induit par Laser (SEPIL), in, Lyon 1, 1999.